Carnets Geol. 26 (5)

E-ISSN 1634-0744
DOI: 10.2110/carnets.2026.2605

Triassic (Rhaetian) El Puquén Formation, Chile: Synsedimentary graben, soft-sediment deformation, volcanism, and U-Pb Zircon ages in a near-arc basin

Manuel SUÁREZ [1, 2]
Jean-Baptiste GRESSIER [1, 3]
Rita DE LA CRUZ [4]

Abstract: The Triassic to Early Jurassic fore-arc basin successions of the coastal region of Central Chile (approximately 32°14' South latitude) form a continuous belt of sedimentary and volcanic rocks, younging to the south. This belt includes, from north to south, the El Quereo, Pichidangui, El Puquén, and Los Molles formations. This note addresses: i) the facies associations and tectonic setting of the El Puquén Formation and the uppermost strata of the underlying Pichidangui Formation, and ii) the first two Rhaetian zircon U-Pb laser-ablation dates of approximately 201 to 208 Ma on volcanic samples from the former, which are younger than the currently accepted Norian-Carnian ages. Basaltic-andesitic lava domes, hyaloclastites and peperites in the uppermost facies of the Pichidangui Formation were emplaced in a subaqueous environment (lacustrine or marine?). Currently these are considered a subduction-related, bimodal volcanic succession synchronous with rifting. Seven facies associations are identified in the conformably overlying lacustrine deposits of the El Puquén Formation, including storm deposits accumulated in a synsedimentary graben approximately 15 m wide, slump deposits, turbidites, pyroclastic intercalations, sedimentary dikes, peperites, and hyaloclastites.

Keywords:

- volcano-sedimentary facies;
- Triassic basin;
- volcanic arc;
- Central Chile;
- U-Pb zircon ages

Citation: SUÁREZ M., GRESSIER J.B. & DE LA CRUZ R. (2026).- Triassic (Rhaetian) El Puquén Formation, Chile: Synsedimentary graben, soft-sediment deformation, volcanism, and U-Pb Zircon ages in a near-arc basin.- *Carnets Geol.*, Madrid, vol. 26, no. 5, p. 107-123. DOI: 10.2110/carnets.2026.2605

Résumé : ***Formation El Puquén (Rhaétien, Trias), Chili : Graben synsédimentaire, déformations de sédiments meubles, volcanisme et datations U-Pb sur zircons dans un bassin proche d'un arc volcanique.-*** La succession géologique du Trias au Jurassique inférieur le long de la côte centrale du Chili forme une ceinture continue de roches sédimentaires et volcaniques avec des faciès variés dans un contexte tectonique lié à la subduction et au rifting. Des datations récentes indiquent que certains volcans seraient d'âge rhétien, plus jeunes que suspecté. Les faciès volcaniques de la Formation Pichidangui, déposés dans un environnement subaquatique, reflètent une activité bimodale associée à la subduction. La Formation El Puquén présente plusieurs associations de faciès lacustres, témoignant d'un environnement dynamique avec des dépôts de tempête, des turbidites, des intercalations pyroclastiques, des dikes et des hyaloclastites, autrefois classés différemment.

Mots-clefs :

- faciès volcano-sédimentaires ;
- bassin triassique ;
- arc volcanique ;
- Chili central ;
- datations U-Pb sur zircons

[1] *Escuela de Ciencias de la Tierra, Faculty of Engineering, Universidad Andres Bello-Viña del Mar (Chile)*

[2] *manuel.suarez@unab.cl*

[3] *jean.gressier@unab.cl*

[4] *Sub-Dirección Nacional de Geología, Servicio Nacional de Geología y Minería, Avda Santa María 0104, Santiago (Chile)*
pepidelacruz@yahoo.es

Published online in final form (pdf) on February 24, 2026
[Editors: José Noel PÉREZ ASENSIO & Beatriz BÁDENAS; language editor: Robert W. SCOTT; technical editor: Bruno R.C. GRANIER]

1. Introduction

Triassic rocks, exceeding 5,000 m in thickness (MORATA *et al.*, 2000), are exposed in the coastal area of central Chile, from Los Molles to Los Vilos (ca. 32° S latitude, Fig. 1). These rocks include continental and marine sedimentary and volcanic deposits that accumulated in southwestern Gondwana (see CECIONI & WESTERMANN, 1968; RIVANO & SEPÚLVEDA, 1991). This thick succession is subdivided into the following formations, listed from base to top (CECIONI & WESTERMANN, 1968; Fig. 1):

1. The El Quereo Formation, of Upper Anisian age based on the presence of *Daonella dubia*, consists of a 713 m-thick succession of basal colluvial breccias (3-4 m thick), fluvial and deltaic (fan delta) deposits, prodelta turbidites and shales, and an upper prodelta facies (SUÁREZ & SEPÚLVEDA in RIVANO & SEPÚLVEDA, 1991). This succession unconformably overlies isoclinally folded metasedimentary beds of the Early Carboniferous Arrayán Formation (CHARRIER *et al.*, 2024). This unconformity is well-exposed a few kilometeres south of Los Vilos.
2. The Pichidangui Formation, an upper Anisian-Norian homoclinal succession (CECIONI & WESTERMANN, 1968), is mainly composed of subduction-related (IBÁÑEZ, 2021), acidic and basic volcanic rocks in a bimodal magmatic suite, synchronous with rifting and locally deposited in a subaqueous environment (VICENTE, 1976; CHARRIER, 1979; MORATA *et al.*, 2000).
3. The El Puquén Formation, which conformably overlies the Pichidangui Formation, is a subaqueous sedimentary succession inferred to be lacustrine, with marine intercalations in its upper levels (CECIONI & WESTERMANN, 1968), and assigned to the Norian (FUENZALIDA, 1938) or Carnian (MELCHOR & HERBST, 2000). CECIONI and WESTERMANN (1968) defined the La Caleta Formation as a fault-bounded unit of volcanic breccias exposed west of Los Molles town. It was included in the Pichidangui Formation (MORATA *et al.*, 2000); however, we consider it as another facies association of the El Puquén Formation following MELCHOR and HERBST (2000); 4) The lower horizons of the Los Molles Formation overlie the El Puquén Formation with a concealed contact inferred to be conformable based on the near parallelism of the beds. These lower strata of the Los Molles Formation, tens of meters thick, underlie beds of the upper horizons of the same formation containing Hettangian ammonites. Therefore, these lower beds are assigned to the Late Triassic (see CECIONI & WESTERMANN, 1968). The Late Triassic to Early Jurassic Los Molles Formation is a deepening marine sedimentary succession approximately 750 m thick (CECIONI & WESTERMANN, 1968; BELL & SUÁREZ, 1995). The bedding of the El Puquén and Los Molles formations is subparallel, forming a shallow-dipping monocline.

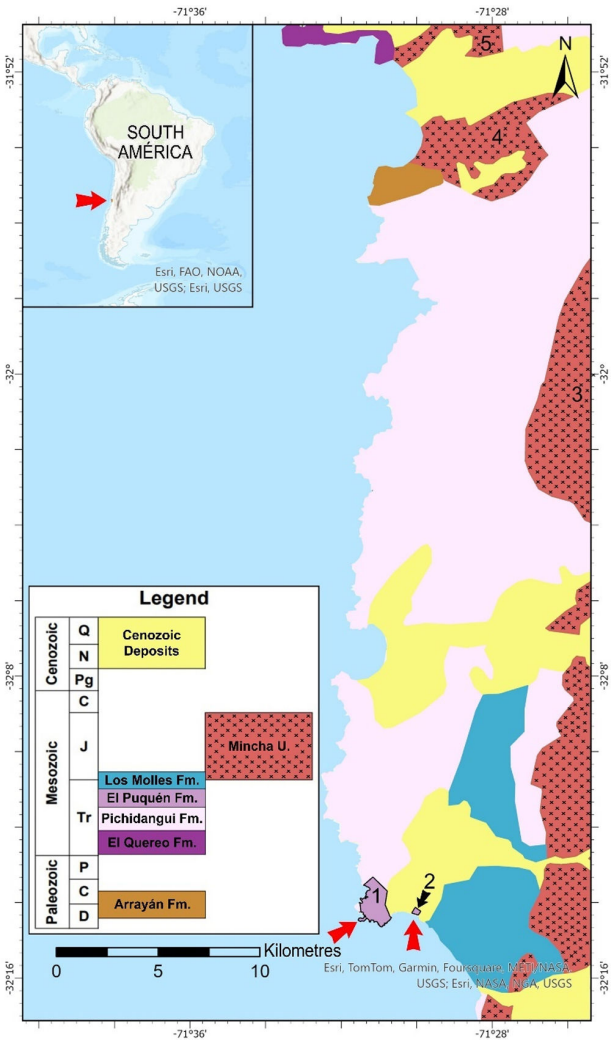

Figure 1: Location map of the section studied in Los Molles, La Ligua, Fifth Region, Chile. Modified from RIVANO and SEPÚLVEDA, 1991; RIVANO *et al.*, 1993. Red arrows show the studied areas. **1:** El Puquén Formation, Los Lobos area (CECIONI & WESTERMANN, 1968), **2:** El Puquén Formation, El Chivato area (CECIONI y WESTERMANN, 1968), **3:** Location of K-Ar 164±4 Ma quartz monzodiorite (ESPIÑEIRA, 1989; RIVANO *et al.*, 1993), in general from 156 to 170 Ma, **4:** Location of Rb-Sr 200±10 Ma (NASI PRADO *et al.*, 1985; BROOK *et al.*, 1986; PARADA *et al.*, 1988) and **5:** Location of Rb-Sr 203±15 Ma (BROOK *et al.*, 1986) and location of K-Ar 173±20 Ma granodiorite (MUNIZAGA, 1972).

These Triassic-Jurassic successions crop out to the south and west of the Mincha Superunit, an Early-Middle Jurassic plutonic association (BROOK *et al.*, 1986; RIVANO & SEPÚLVEDA, 1991; Fig. 1). Rifting during the Triassic in southwestern Gondwana has been widely proposed by several authors (*e.g.*, CHARRIER, 1979; BELL & SUÁREZ, 1995); however, "the extensional faults that control the basins in Chile have not been clearly identified" (see CHARRIER *et al.*, 2014). In this note, we present data supporting synsedimentary extensional tectonism at the base of the El Puquén Formation, complemented by facies studies indicative of intra- and fore-arc deposition. The Late Triassic age previously assigned to these rocks, based on stratigraphic and paleontological data (FUENZALIDA, 1938; AZCÁRATE & FASOLA, 1970; TRONCOSO & HERBST,

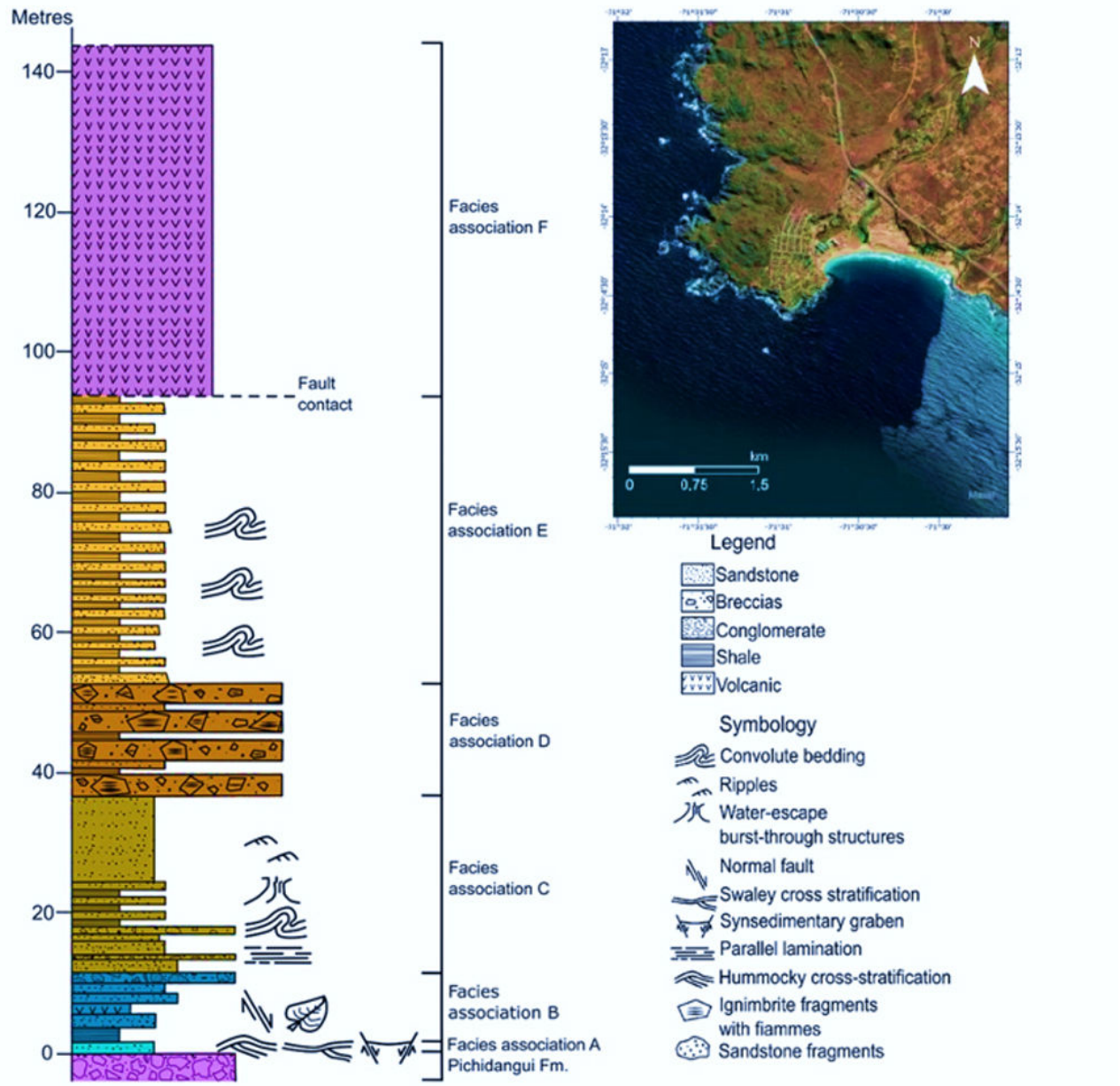

Figure 2: Facies associations of the El Puquén Formation. Inset, Google satellite image of the studied area.

1999; Melchor & Herbst, 2000; Herbst & Troncoso, 2014), is corroborated here by two new laser-ablation U-Pb zircon dates. This article also contributes to the understanding of the geology of an area that, despite being a classic locality with excellent exposures of Upper Triassic and Lower Jurassic sedimentary and volcanic rocks located near major cities such as Santiago and Viña del Mar, has a limited geological literature (Fuenzalida, 1938; Cecioni & Westermann, 1968; Azcárate & Fasola, 1970; Bell & Suárez, 1995; Melchor & Herbst, 2003; Suárez *et al.*, 2018).

2. Stratigraphy

The main stratigraphic elements of the upper strata of the Pichidangui Formation, the El Puquén Formation, and the lower horizons of the Los Molles Formation are presented in Figure 2.

i. The uppermost facies of the Pichidangui Formation

The Pichidangui Formation is a subduction-related volcanic succession (Ibáñez, 2021) comprising basalts, andesitic basalts, rhyolites, and dacites (Vergara *et al.*, 1991; Cancino, 1992; Ibáñez, 2021). It is up to 4,000 to 5,000 m thick, exhibiting a bimodal magmatic pattern inferred to be synchronous with rifting (Morata *et al.*, 2000). "Marine sedimentary rocks predominate in its lower section, whereas rocks characteristic of paralic conditions of sedimentation are found at the top, where temporary continental conditions are reported" (Cecioni & Westerman, 1968; Vicente, 1976; Charrier, 1979; Vergara *et al.*, 1991, 1995; Morata *et al.*, 2000). The upper horizons of the Pichidangui Formation are primarily products of hydrovolcanism, including hyaloclastites and peperites (Fig. 3) (Suárez *et al.*, 2018; Ibáñez, 2021).

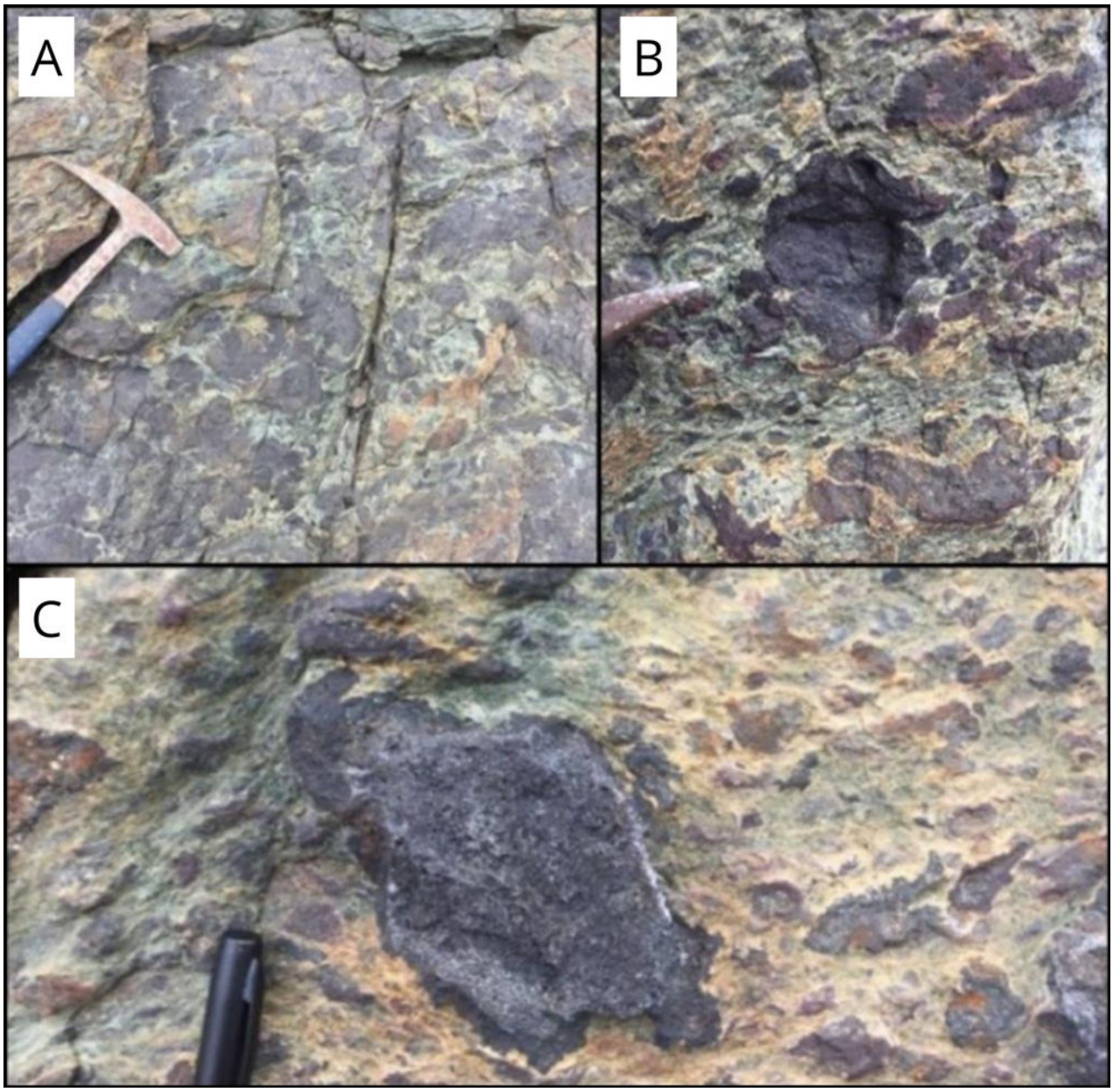

Figure 3: Volcaniclastic deposits of the Pichidangui Formation at the El Puquén area: **A)** hyaloclastite; **B)** volcanic fragment interpreted as a bomb showing a form due to aerodynamic shaping during rotation; **C)** fragment with a darker rim (probably a chilled margin).

Some of the volcaniclastic beds exhibit fragments with morphology interpreted as the result of subaerial bombs (Fig. 3.B-C) Other fragments resemble cauliflower bombs. Coherent andesitic-basaltic rocks and possible pillow lavas have also been reported (Ibáñez, 2021). The uppermost beds assigned to the Pichidangui Formation are clast-supported conglomerates, pervasively silicified. The clasts are interpreted as fragments of ignimbrites based on the macroscopic identification of fiamme-like structures, which, however, could not be corroborated in thin-section due to intense silicification.

ii. El Puquén Formation

Upper Triassic sedimentary rocks exposed in three separate areas near the town of Los Molles were assigned to the El Puquén Formation by Cecioni and Westermann (1968; Fig. 1). From north to south, these are: i) a succession of approximately 27.5 meters of minimum thickness (Melchor & Herbst, 2000) on the continental coast northeast of Los Lobos Island, and in fault contact with the Pichidangui Formation; ii) the sedimentary strata overlying the Pichidangui Formation, cropping out from a few tens of meters south of El Puquén up to the northern side of the Los Molles beach, and iii) exposures cropping out between the Estero Los Molles and Estero El Chivato, partly in the area of the present-day El Chivato camp site, with a thickness of 200 m (Cecioni & Westermann, 1968). These authors indicate a total thickness of 500-1,000 m for these rocks. A succession of mainly monolithologic volcanic breccias, which were included in the La Caleta Formation by Cecioni and Westermann (1968), is herein tentatively incorporated as another facies (facies F) of the El Puquén Formation. Initially, these au-

Table 1: Facies association of the El Puquén Formation.

Late Triassic paleoenvironments of the upper Pichidangui, El Puquén and lower Los Molles formations				
Los Molles Formation	Basal Member	Subaqueous delta-front paleochannels in a fore-arc basin		Fore-arc basin
El Puquén Formation	Fag	Shales, sandstones and lapilli air-fall deposits	Late Triassic marine transgression and distant explosive volcanism	Near-arc lacustrine-marine basin
	Faf	Subaqueous hydrovolcanism and surtseyan volcanoes indicated by hyaloclastites and air-fall pyroclasts		Intra-arc lacustrine basin
	Fae	Basin floor accumulation of sandstones alternance alternating with shales, near the roots of volcanoes as indicated by the peperite dikes emplaced in shales		Near-arc lacustrine basin
	Fad	Heterogenous, mixed-up pyroclastic flow, accumulated in the basin floor, thin-bedded turbidites	Slope apron	Near-arc lacustrine basin
	Fac	Slope-apron facies with mass flow deposits, slumps, olistolith, synsedimentary dikes, convolute bedding	Synsedimentary deformed sediments	
	Fab	Deeper lake accumulation as suggested by the predominance of dark shales, probably anoxic as inferred from the absence of trace fossils, with air-fall tuff intercalations. Thin bedded turbidites	Post-graben, during extensional tectonism	Near-arc lacustrine basin
	Faa	Storm-prone, shallow lacustrine environment as indicated by hummocky cross laminations and the inverse to normally graded pyroclastic-rich sandstones interpreted as tempestites	Synsedimentary graben	Near-arc lacustrine basin
Pichidangui Formation		Subaqueous volcanoes, occasionally emerging above the water-surtseyan volcanoes in an intra-arc basin		Intra-arc basin

thors suggested that the latter beds were deposited in a Carboniferous glaciolacustrine environment; however, CECIONI later referred them to the Middle? Triassic based on the presence of plant remains assigned to that age (in STIPANICIC, 1983, see MELCHOR & HERBST, 2000).

The thinly-bedded shales and fine-grained sandstones exposed in the El Chivato camp site resemble some of the Los Molles Formation strata, but in this work are incorporated in the El Puquén Formation (as Facies association G) based on the presence of lapilli air-fall intercalations considering the absence of pyroclastic beds in the Los Molles Formation. This facies association is in turn overlain, with a covered contact-probably conformably, considering the near parallelism of the beds-by the Los Molles Formation exposed to the south. The lower beds of the Los Molles Formation at this locality include two paleochannels filled with quartz-rich conglomerates separated by shale and fine-grained sandstone, some with hummocky cross bedding. MELO (2020) interpreted these beds as a subaqueous facies of a delta system. Hettangian ammonites (CECIONI & WESTERMANN, 1968), in fine-grained sandstones tens of meters stratigraphically above these paleochannels, suggest a Late Triassic age for these basal beds. Higher up in the Los Molles Formation, trace fossils indicate a shallow sea (COVACEVICH *et al.*, 1987), followed by deepening of the basin with contourites and turbidites that thicken stratigraphically upwards. Some of these facies and the presence of slump horizons have been interpreted as representing slope-trench deposits by BELL and SUÁREZ (1995).

A Late Triassic Triassic age for the El Puquén Formation is confirmed here by U-Pb zircon laser-ablation dating (see below). The base of the El Puquén Formation is marked by the first sandstone overlying, apparently in conformity, a clast-supported conglomerate composed of subrounded silicified clasts interpreted as fragments of ignimbrites. The latter is based on the presence of fiamme-like structures, measuring ca. 5 cm in length and assigned herein to the Pichidangui Formation.

Seven facies associations are recognized in the El Puquén Formation (Fig. 2; Table 1).

iii. Facies association A: Syn-tectonic graben sedimentary fill

A syn-extensional tectonic sedimentary succession, 160 cm-thick, forms the base of the El Puquén Formation approximately 200 meters south of the El Puquén site. It conformably overlies a clast-supported conglomerate composed of subrounded silicified clasts of ignimbrites, which are assigned herein to the Pichidangui Formation. From base to top, these beds include a 40 cm-thick layer with hummocky and swaley cross-stratification in fine-grained sandstones, with laminae thickening into swales and thinning over hummocks, with a wavelength of approximately 100 cm (Fig. 4.A). These strata are overlain by grey parallel-laminated shale, 8 cm-thick, and two pyroclastic-rich, coarse volcanic sandstones, 10-20 cm in thickness, that exhibit normal grading (Fig. 4.B-C). These sediments are interpreted as having formed in shallow waters by storms (tempestites), although heavy waves due to volcanism in coastal areas might also generate similar sedimentary structures. These strata were deformed by a pair of well-developed extensional faults while the sediments were still unconsolidated, resulting in the formation of a synsedimentary graben (Fig. 4.D). The graben is flanked by normal faults, exposed along a 30 meters length, with attitudes of 120/60 (strike/dip) (the western fault) and 074/45 (the eastern fault), separated

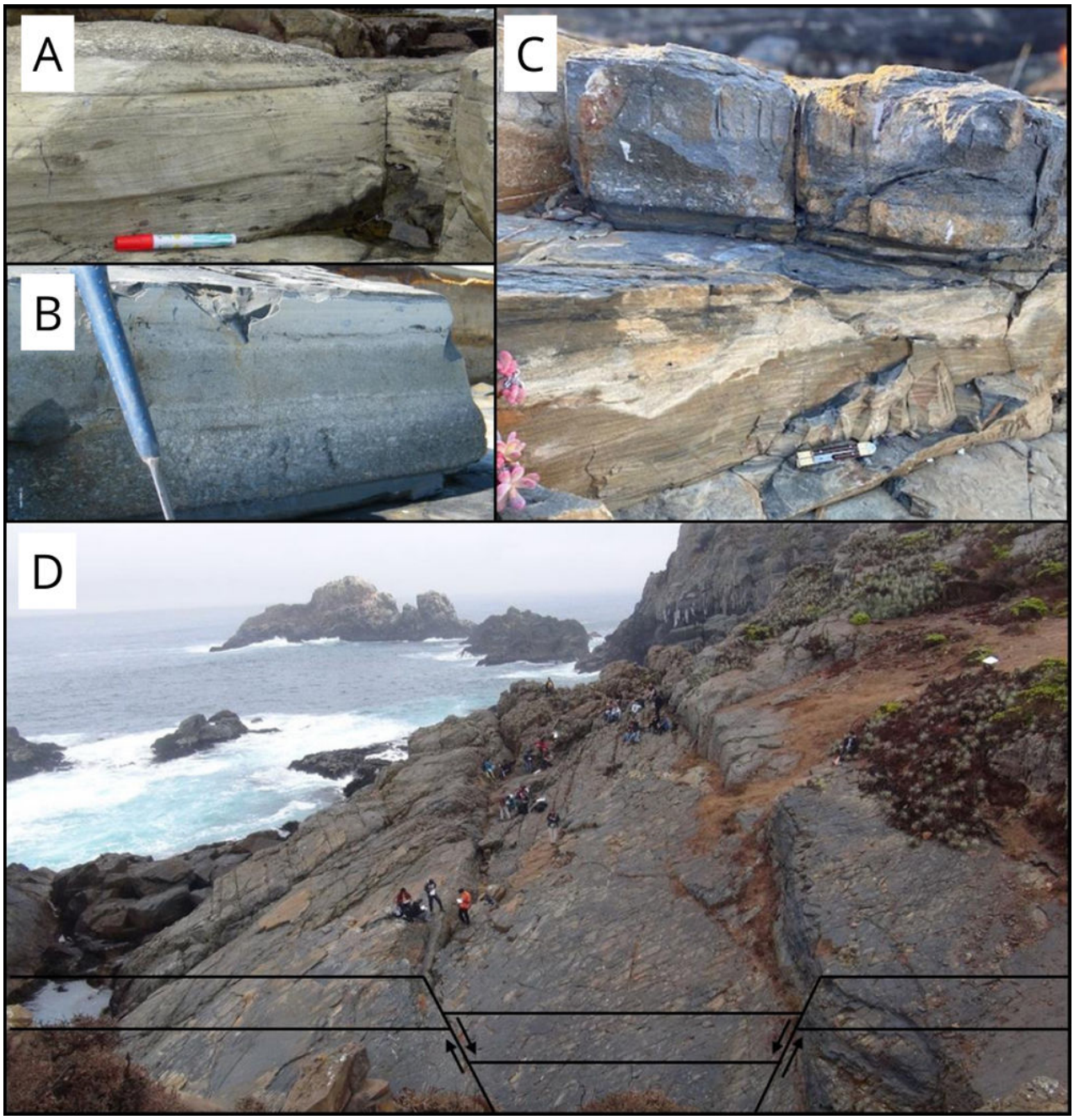

Figure 4: A) Hummocky and swaley cross stratification in fine grained sandstones with laminae thickening into swales and thinning over hummocks, overlain by coarse grained volcanic sandstone locally with reverse to normal grading (tempestites); **B-C)** parallel-laminated shales, that exhibit normal grading; **D)** synsedimentary graben bounded by normal faults separated by approximately 13-15 meters, with a vertical throw of less than 2 meters.

by a distance of up to 15 m. These are scissor faults, covered by low-angle dipping sedimentary beds of facies association B. This depositional contact supports the synsedimentary nature of the graben. The western fault shows a variable displacement along the fault, with a westward increasing offset from an initial point of no offset (Fig. 5.A). The faulted sedimentary rocks exhibit a gradual change from folding above the fault to no deformation at the initial point of no offset (Fig. 5.B). At the point of no offset, the beds of facies association B cover the fault with no deformation (Fig. 5.C).

iv. Facies association B: Post-graben thin-bedded turbidites, tuffs, and synsedimentary faults

A 10 m thick succession of alternating dark grey shales, sandstones, normally graded thin volcanic sandstones, and thin light grey tuff intercalations covers the synsedimentary faults of the graben (Fig. 6.A). Healed and short (less than 4 m in length) normal faults cut through these beds (Fig. 6.B). The main sedimentary beds within this facies association are (Fig. 6): i) Thin parallel-laminated and massive dark shales, less than 2 cm thick, in horizons ranging from 3 to 210 cm

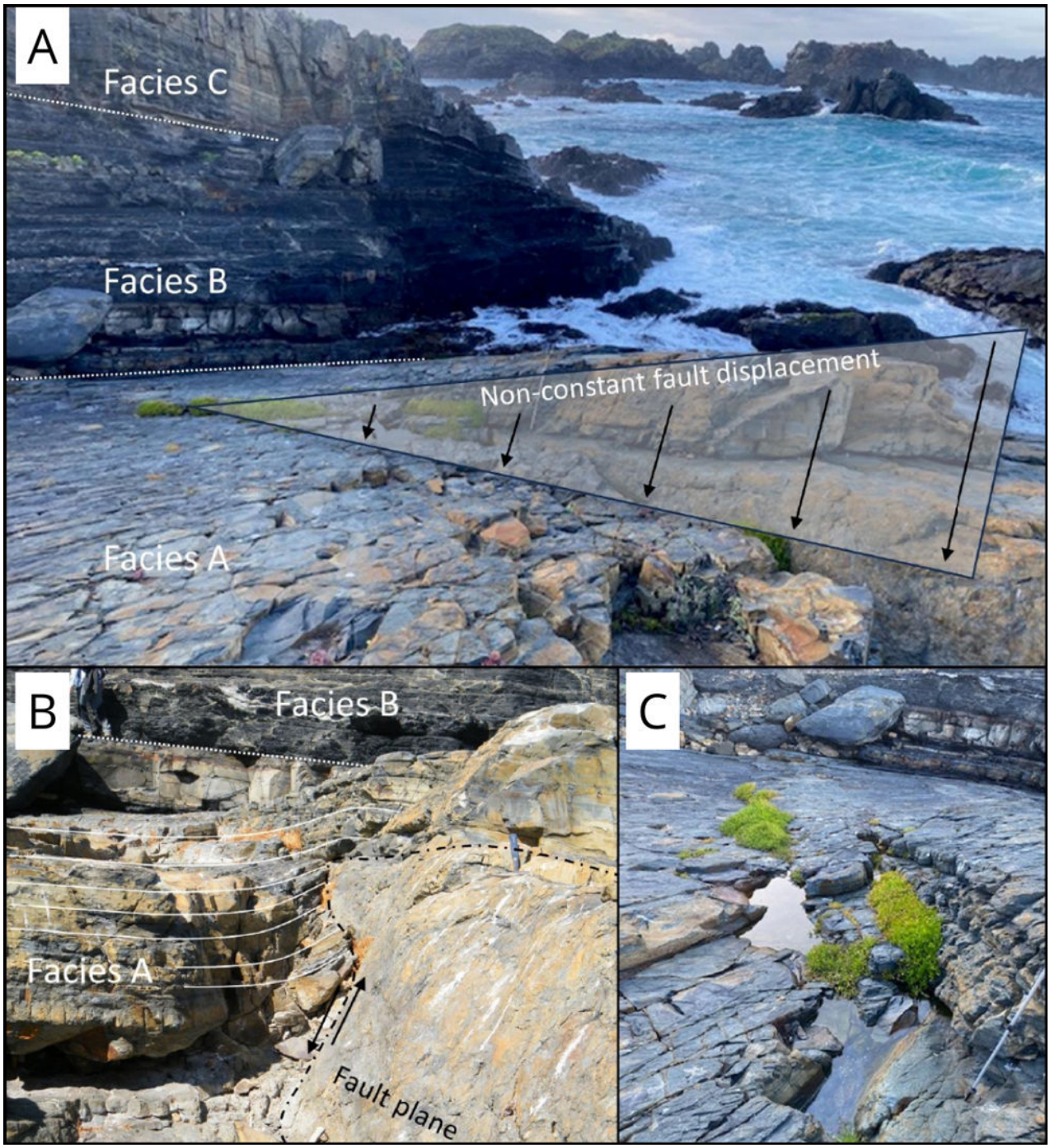

Figure 5: A) scissor fault shows variable displacement along the fault from an initial point of no offset; **B)** sedimentary beds draping the fault and gradual upward decreasing of the dip of the faulted sedimentary strata; **C)** blanketing of the fault by overlying beds of facies association B.

thick, some with fossil plant remains (CECIONI & WESTERMANN, 1968); ii) Thin- and medium-bedded (1-10 cm thick), normally graded and massive fine to medium-grained turbidites, some with mud flakes (Fig. 6.C); iii) White airfall pyroclastic intercalations, 1-4 cm thick (Fig. 6.A); iv) Parallel-laminated sandstones; v) Synsedimentary breccia with rip-up fragments of shale (Fig. 6.D). Dewatering features are locally present: load casts, initially interpreted as originating from currents (the flames of Plate I, fig. 1 of CECIONI & WESTERMANN, 1968) and convolute bedding, some overturned (Fig. 6.E-F). The absence of any signs of trace fossils in the dark shales may suggest an anoxic environment in a relatively deep lake environment, where turbidites and ash falls accumulate.

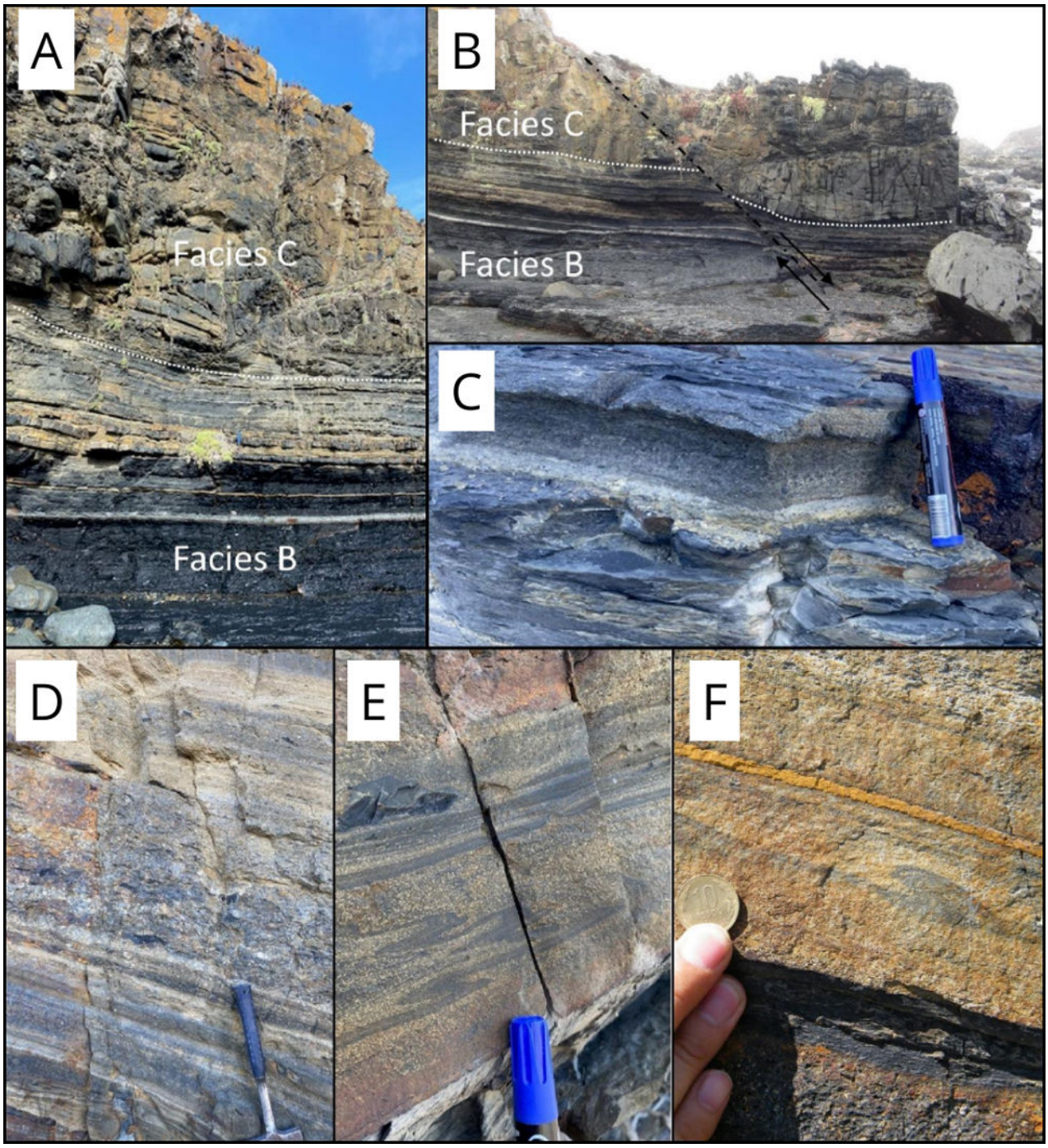

Figure 6: A) coarse synsedimentary breccia at the base of facies association C overlying a thin-bedded succession of facies association B; **B)** thin- and medium- bedded turbidites, shale, white thin layers of ash-fall tuff of facies association B, covered by synsedimentary coarse breccias of facies association C, with a small healed synsedimentary normal fault cutting both facies associations; **C)** thinly bedded normal and inverse to normally graded volcaniclastic turbidites; **D),** synsedimentary breccia with rip-up fragments of shale; **E)** overturned convolute bedding; **F)** flame-load-cast at the base of thin-bedded turbidite (see Plate I, fig. 1 of CECIONI & WESTERMANN, 1968).

v. Facies association C: A slumped succession (Fig. 7)

This facies association, approximately 25 m thick, is mainly formed by mass flow and slumped deposits (Fig. 7.A). It conformably overlies facies association B (lower strata in Fig. 6.A), with a 470 cm thick basal horizon, of coarse-grained sandstones, granule conglomerates, some filling paleochannels, parallel-laminated sandstones, and synsedimentary breccias. These beds are commonly contorted and formed by slumped beds (Fig. 7.A). Some facies of this association are an olistolith (Fig. 7.B); c) Slumped sediments, including folded beds and synsedimentary breccias; d) A sedimentary dike probably formed by overpressure related to the superposition of slumped beds on sedimentary strata or by seismicity associated with volcanic eruptions (Fig. 7.D); e) Convolute bedding and water-escape burst-through structures at the top of sandstone turbidites (Fig. 7.C).

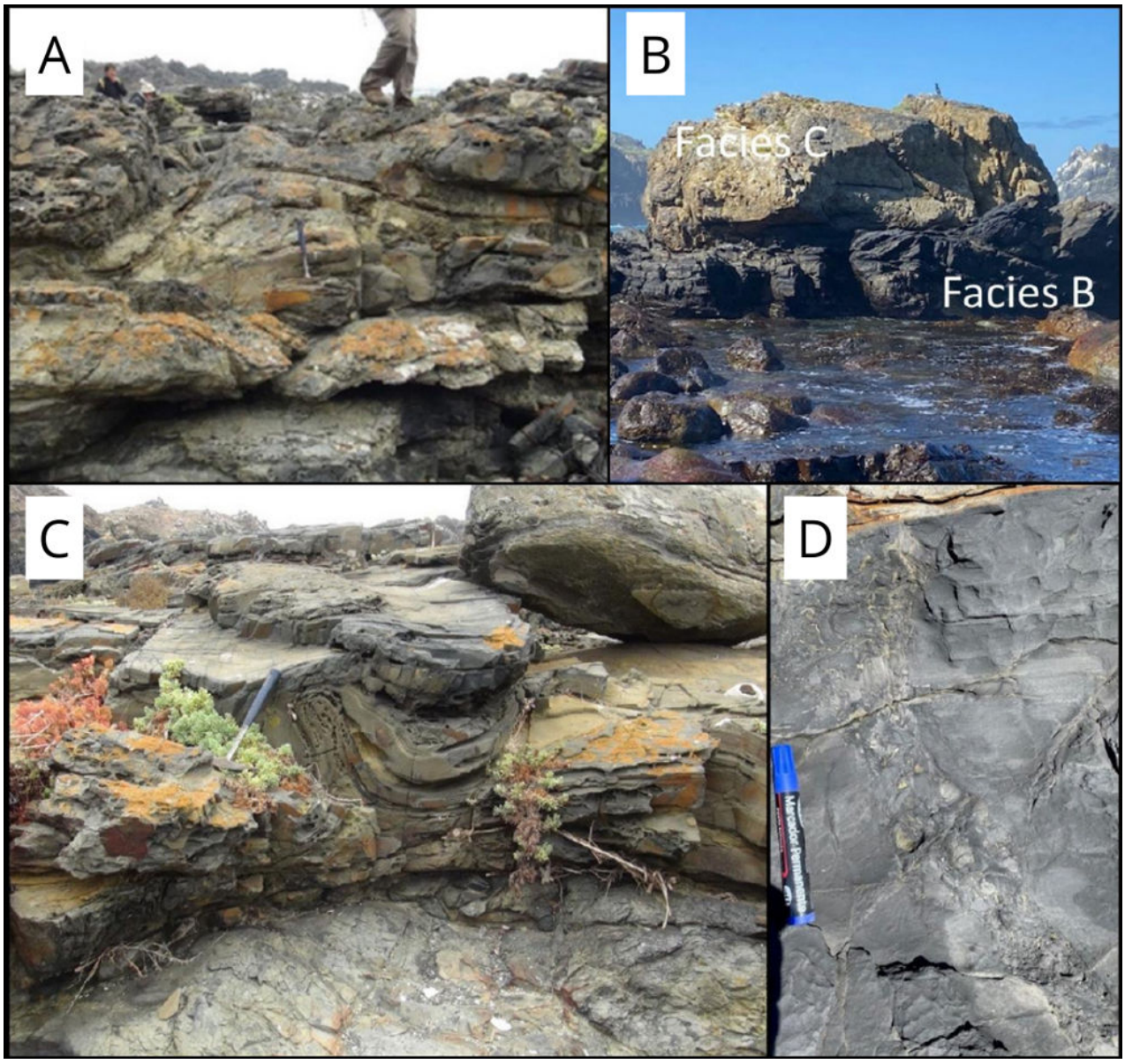

Figure 7: A) slumped beds; **B)** olistolith; **C)** convolute bedding; **D)** synsedimentary dike of facies C.

vi. Facies association D: Brecciated ignimbrite and thin-bedded turbidites

Facies association D is separated from the rest of the succession to emphasize the presence of a heterogeneous breccia, including large boulders of ignimbrite fragments with fiammes (1.5 x 2.0 m), shales, and stratified sandstone layers 30 cm-long (Fig. 8.A-B). This bed is interpreted as the result of mixing between a pyroclastic flow and unconsolidated and semiconsolidated sediments on the floor of a lacustrine basin. The underlying sedimentary beds are deformed, probably due to overpressure generated by the arrival of the pyroclastic flow while the sediments were still wet. A Late Triassic U-Pb zircon laser ablation date from a sample of these rocks is presented in this note (sample LMM-4, see below).

vii. Facies association E: Peperite dikes emplaced in shales and sandstones

Facies association E is a ca. 40 m-thick succession conformably overlying facies association D and is composed of alternating shales and massive and normally graded sandstones (10-150 cm thick), interpreted as turbidites, with occasional convolute bedding, and synsedimentary breccias with rip-up shale fragments. This succession was intruded by peperite dikes (Fig. 8.C-D). Some of these dikes are tabular, 4 m wide, with a NW trend, while others are irregular in shape. Synsedimentary dikes, 10-40 cm thick, developed along some of the contacts of the peperite dikes with the cover rocks. These synsedimentary dikes were likely formed as a result of processes related to the emplacement of the peperites.

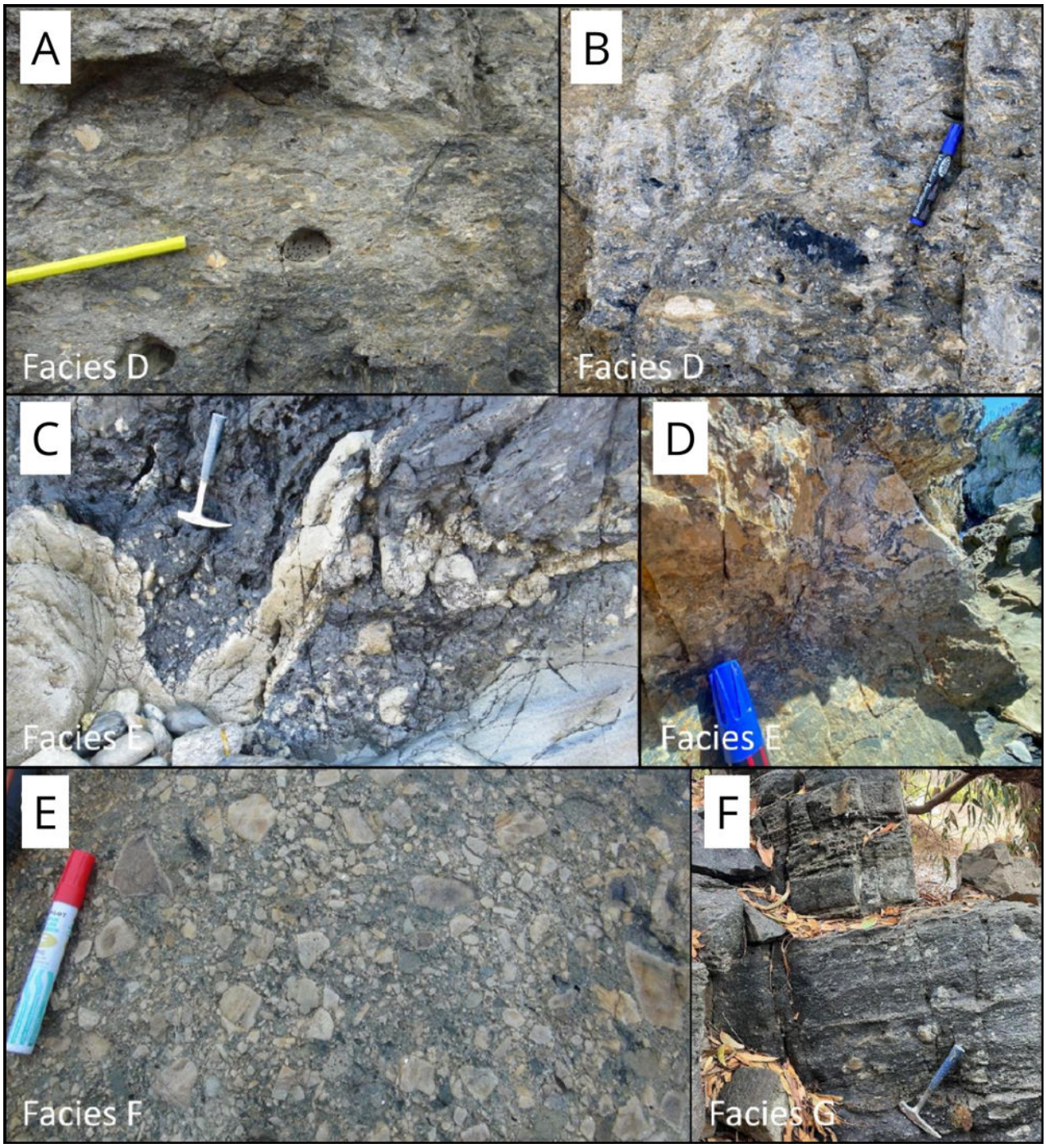

Figure 8: A-B) heterogeneous breccia of facies association D, with intermingling of ignimbrite blocks with eutaxitic foliation and sedimentary fragments (A) and shale inclusions in the breccia (B); **C)** peperite dike emplaced in fine and medium-grained sandstones and shales; **D)** brecciation of margin of peperite dike, **E)** monolithologic volcanic breccia interpreted as hyaloclastites, weakly foliated of facies association F; **F)** thinly bedded sandstones and shales with intercalations of monolithologic lapilli beds of the facies association G.

viii. Facies association F: Hydrovolcanic facies association "La Caleta Formation"

A succession of monolithologic volcanic breccias, in fault contact with facies association E, included in the La Caleta Formation by CECIONI and WESTERMANN (1968), is tentatively incorporated herein as a distinct facies of the El Puquén Formation. The contact fault is poorly exposed, which prevented the identification of its nature and any inference about stratigraphic relationship of both facies associations. A sedimentary structure shown in a photograph from this succession was published by CECIONI and WESTERMANN (1968: Pl. I, fig. 2, p. 55) who interpreted it as resulting from "isolated angular pebbles which apparently tumbled down as a 'rain' on the unconsolidated very fine laminated limy-sandy sediment, so that in sinking, the laminae were moulded around it. This phenomenon suggests rafting, possibly by floating ice." Based on this interpretation, CECIONI and WESTERMANN (1968) suggested a Carboniferous age for these strata, considering the glaciation of that time. However, the timing of these strata was revised when Late Triassic fossil leaves were found

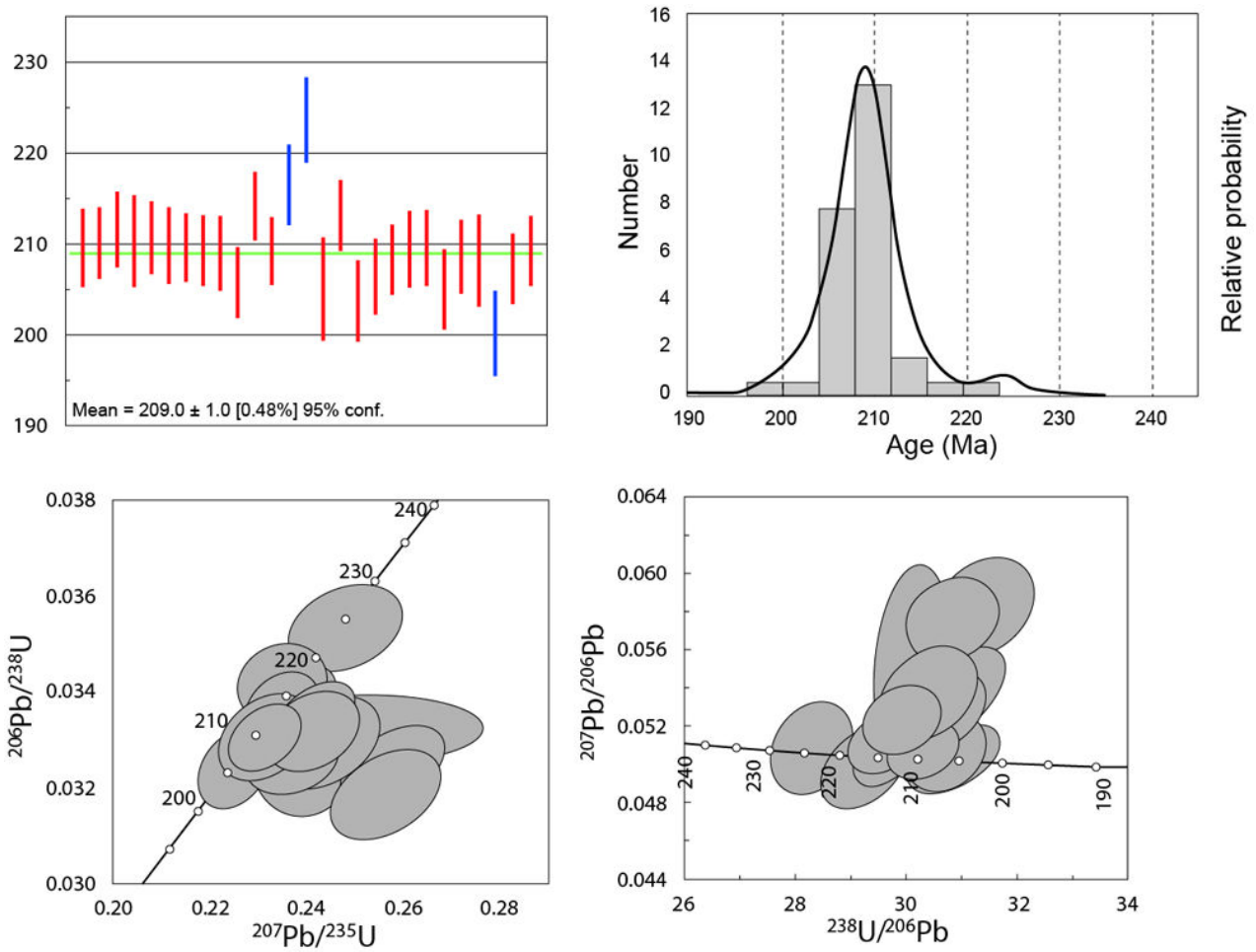

Figure 9: Radiogenics ages of sample LMM-4.

(CECIONI in STIPANICIC, 1983, 2001). Our interpretation of this structure is of an impact-sag feature caused by a volcanic bomb in the non-lithified bottom sediment of the El Puquén Formation basin. Most of the coastal exposures of this facies association are monolithologic volcanic breccias, interpreted herein as hyaloclastites (Fig. 8), probably the products of surtseyan volcanism. A Late Triassic U-Pb zircon laser ablation date from a sample of these rocks is presented in this note (sample LMM-6, see below).

ix. Facies association G: Subaqueous shales, sandstones, and lapilli tuff intercalations

A succession of thinly bedded sandstones and shales with 60 cm-thick intercalations of monolithologic lapilli beds, 200 m-thick, representing air-fall deposits, and exposed between Estero Los Molles and Estero El Chivato (at the El Chivato camping site), represents the southern beds assigned to the El Puquén Formation (Fig. 8.E). Although an area with no outcrops separates these strata from those of Facies F to the north and from the base of the Los Molles Formation to the south, they are interpreted as the youngest association of this formation (CECIONI & WESTERMANN, 1968), based on the general southward younging succession of the El Puquén Formation. The latter authors indicated that "the interbedding of plant-bearing beds with sediments bearing marine faunas ['Los Molles flora' and 'Nevadites' (Sandlingites) of FUENZALIDA, 1938] suggests alternation between lacustrine and marine environments." An area with no exposure separates these beds from the overlying Los Molles Formation. This association is lithologically similar to the basal facies of the Los Molles Formation, except for the distinct lapilli-tuff intercalations.

3. Zircon U-Pb geochronology

i. Methodology

The Laser Ablation Zircon U-Pb analyses were conducted at the Isotopic Geology unit of the Servicio Nacional de Geología y Minería (SERNAGEOMIN), Chile (laboratorios@sernageomin.cl). The U-Pb dating method using laser ablation inductively coupled plasma mass spectrometry (LA-ICP-MS) was conducted by F. LLONA, Marco SUÁREZ, and A. BUSTOS. Sample preparation involved crushing, grinding, and obtaining fragments of less than 500 μm, followed by the concentration of heavy minerals using a Gemini table, leading to the manual separation of zircons under UV light or dense liquids. Zircons were mounted on a 2.5 cm diameter epoxy resin briquette, polished to expose the crystal interiors, with 30 to 120 crystals installed per sample depending on the dating objectives. Cathodoluminescence images were obtained to identify internal zircon structures, and

backscattered electron images visualized fractures and inclusions, using a Zeiss MA-10 scanning electron microscope. The briquettes were then placed in a Photon Machines Analyte 193.G2 laser ablation system, with standards GJ-1. The resulting material was transported via helium and argon gases to a Thermo Fischer Element XR mass spectrometer for isotope measurement. Data reduction was performed with Iolite software, with isotopic fractionation and instrumental drift corrected using the primary standard. Secondary standards were treated as unknowns for quality control. Final age results were calculated and organized using the Isoplot add-in for Microsoft Excel, employing constants adopted from the 25th International Geological Congress in 1976, Sydney, Australia, subsequently published by STEIGER and JÄGER (1977) [$\lambda(^{238}U)=1.55125x10^{-10}$ year^{-1}, $\lambda(^{235}U)=9.8485x10^{-10}$ year^{-1}, atomic ratio $^{238}U/^{235}U=137.88$].

ii. Sample description and age

Two samples of igneous rocks from the El Puquén Formation were analyzed:

- Sample LMM-4 (262242-6430389) is from an ignimbrite fragment from a synsedimentary volcaniclastic breccia from facies association E, interpreted as the result of the collapse of a pyroclastic flow along the slope of a lake, incorporating shales and sandstones as rip-up fragments. Twenty-seven zircon grains were analyzed that gave $^{206}Pb/^{238}Pb$ ages of 223±4.7 to 200.1±4.7 Ma (Fig. 9, Table 2). The youngest nine gave a near-Rhaetian age ranging from 208.3±3.8 to 200.1±4.7 Ma, interpreted as autocrystic zircons, formed near the eruption time. Older Norian radiometric ages ranging from 209.2±3.7 to 223.5 ±4.7 Ma, with a weighted mean of the $^{206}Pb/^{238}U$ ages for 24 analyses gave a Norian age of 209 ±1.0 Ma, may represent antecrystic grains from "slightly" older magmas.
- Sample LMM-6 (262341-6430199) was taken from a hyaloclastite breccia of facies association F. Twenty-six zircon grains were analysed that gave $^{206}Pb/^{238}Pb$ ages of 296.0±7.5 to 200.5±2.7 Ma (Fig. 10, Table 3). The five youngest zircon grains gave a Rhaetian age ranging from 208.1±4.4 to 200.5±2.7 Ma, interpreted as autocrystic zircons and indicative of the eruption age. Twenty grains gave Norian ages ranging from 209.0±4.3 to 226.9±5.1 Ma, with a weighted mean of the $^{206}Pb/^{238}U$ ages giving a Norian age of 211.70 ± 2.61-2.64 Ma, may represent antecrystic grains

Table 2: Sample LMM-4.

				Radiogenic							Ages (Ma)						Corrected Ages (Ma)		
Grain. Spot	U (ppm)	Pb (ppm)	Th (ppm)	$^{207}Pb/^{235}U$	±	$^{206}Pb/^{238}U$	±	rhoc	$^{207}Pb/^{206}Pb$	±	$^{207}Pb/^{235}U$	±	$^{206}Pb/^{238}U$	±	$^{207}Pb/^{206}Pb$	±	$^{206}Pb/^{238}U$	±	$^{207}Pb/^{206}Pb$
1	54	18	37	0.2409	0.0083	0.0332	0.0007	0.1840	0.0543	0.0017	219.1	6.7	210.6	4.2	303	60	209.6	4.3	0.84944
2	128	64	139	0.2355	0.0073	0.0332	0.0006	0.1617	0.0522	0.0015	214.7	5.7	210.6	4.0	247	52	210.1	4.0	0.84944
3	77	30	65	0.2415	0.0070	0.0334	0.0007	0.4862	0.0524	0.0012	219.6	5.6	212.1	4.1	290	49	211.6	4.1	0.84954
4	103	42	87	0.2388	0.0080	0.0333	0.0008	0.4315	0.0528	0.0013	217.5	6.5	210.9	5.0	286	49	210.3	5.1	0.84946
7	174	118	254	0.2425	0.0056	0.0333	0.0006	0.4633	0.0532	0.0010	220.5	4.5	211.5	4.0	311	39	210.7	4.0	0.84950
8	57	23	52	0.2311	0.0076	0.0331	0.0007	0.3628	0.0513	0.0015	211.1	6.2	210.0	4.2	242	58	209.8	4.3	0.84940
9	60	22	47	0.2520	0.0200	0.0332	0.0006	0.0620	0.0546	0.0032	228.2	6.6	210.7	3.7	257	59	209.6	3.8	0.84945
10	150	72	158	0.2333	0.0057	0.0331	0.0006	0.4794	0.0521	0.0010	212.9	4.7	209.8	3.8	278	42	209.3	3.9	0.84938
11	92	49	108	0.2365	0.0066	0.0330	0.0007	0.4589	0.0523	0.0012	215.5	5.3	209.5	4.2	291	48	209.0	4.1	0.84936
12	55	18	38	0.2368	0.0078	0.0326	0.0006	0.2495	0.0541	0.0016	215.8	6.3	206.8	3.9	334	56	205.8	3.9	0.84918
13	135	74	158	0.2385	0.0060	0.0338	0.0006	0.3765	0.0518	0.0011	217.2	4.8	214.6	3.7	260	44	214.2	3.7	0.84971
14	157	74	163	0.2339	0.0053	0.0330	0.0006	0.4675	0.0517	0.0010	213.4	4.4	209.6	3.7	262	40	209.2	3.7	0.84937
15	65	24	51	0.2350	0.0075	0.0342	0.0007	0.1544	0.0515	0.0016	214.3	6.0	216.6	4.4	209	58	216.3	4.5	0.84984
16	59	25	49	0.2481	0.0095	0.0353	0.0008	0.3065	0.0521	0.0018	225.0	7.6	223.9	4.7	268	67	223.5	4.7	0.85034
17	115	66	138	0.2392	0.0084	0.0325	0.0009	0.0756	0.0555	0.0019	217.8	6.2	206.4	5.6	335	59	205.0	5.6	0.84915
18	113	50	106	0.2351	0.0063	0.0336	0.0007	0.2595	0.0516	0.0012	214.4	5.1	213.3	4.0	236	48	213.0	4.1	0.84962
19	68	29	58	0.2577	0.0088	0.0324	0.0007	0.4669	0.0581	0.0016	232.8	7.0	205.8	4.5	506	59	203.8	4.5	0.84911
20	64	23	50	0.2275	0.0081	0.0326	0.0007	0.3398	0.0520	0.0016	208.1	6.5	206.9	4.2	262	59	206.4	4.2	0.84919
21	126	62	135	0.2368	0.0063	0.0329	0.0006	0.3687	0.0521	0.0012	215.8	5.1	208.8	3.8	279	49	208.3	3.8	0.84931
22	104	44	97	0.2302	0.0060	0.0331	0.0007	0.4435	0.0516	0.0010	210.3	4.9	209.8	4.2	240	40	209.4	4.2	0.84938
23	130	64	141	0.2311	0.0062	0.0331	0.0007	0.4133	0.0515	0.0012	211.1	4.9	209.8	4.1	237	47	209.5	4.1	0.84939
24	193	109	242	0.2249	0.0060	0.0324	0.0007	0.3137	0.0518	0.0011	206.0	4.9	205.5	4.4	225	41	205.1	4.4	0.84910
25	82	31	66	0.2309	0.0068	0.0329	0.0007	0.4287	0.0517	0.0012	210.9	5.5	208.9	4.0	252	47	208.6	4.1	0.84933
26	83	34	75	0.2439	0.0093	0.0330	0.0008	0.3518	0.0535	0.0018	221.6	7.4	209.0	5.0	340	71	208.2	5.0	0.84933
27	53	17	31	0.2563	0.0093	0.0319	0.0008	0.3998	0.0587	0.0019	231.7	7.5	202.2	4.8	494	65	200.1	4.7	0.84887
28	54	20	43	0.2304	0.0080	0.0327	0.0006	0.2606	0.0514	0.0016	210.5	6.4	207.6	3.8	251	61	207.3	3.8	0.84924
30	116	51	110	0.2336	0.0063	0.0330	0.0006	0.4231	0.0517	0.0012	213.1	5.2	209.6	3.8	272	48	209.2	3.8	0.84937

from an older crystallization from the same magma and/or as inherited zircons derived from older magmas. Six Permian ages ranging from 289.0± 6.2 to 296.0±7.5 Ma, represent some inherited zircons from older rocks (Table 3).

4. Conclusions

- Triassic regression-transgression episodes. The subaqueous environment of the El Puquén and Los Molles formations is evident. The absence of marine fossils in the El Puquén Formation and the presence of fossil leaves suggest a lacustrine setting, except for the inferred uppermost unit (facies association G), where CECIONI and WESTERMANN (1968) "suggest alternation between lacustrine and marine environments." The latter would represent the transition to the marine deposition of the overlying Late Triassic to Early Jurassic marine succession of the Los Molles Formation. This marks the second Triassic regression-transgression episode in the region, following an earlier episode characterized by fan delta to prodelta marine turbidites represented by the El Quereo and possibly the Pichidangui formations (RIVANO & SEPÚLVEDA, 1991).

- Rhaetian age. Two new U-Pb zircon laser ablation dates from specimens in facies associations D and F of the El Puquén Formation indicate a Rhaetian age ranging from 208 to 200 Ma for this unit. This age is younger than the Late Ladinian-Carnian age indicated by MELCHOR and HERBST (2000) and the Norian age based on fossil flora and the presence of the cephalopod Sandlingites described by FUENZALIDA (1938) and accepted by CECIONI and WESTERMANN (1968). These coeval Rhaetian ages from facies C and E support the inclusion of the latter succession, previously defined as the La Caleta Formation by CECIONI and WESTERMANN (1968), within the El Puquén Formation.

Table 3: Sample LMM-6.

		Radiogenic							Ages (Ma)						Corrected Ages (Ma)		
Grain. Spot	U (ppm)	$^{207}Pb/^{235}U$	±	$^{206}Pb/^{238}U$	±	rhoc	$^{207}Pb/^{206}Pb$	±	$^{207}Pb/^{235}U$	±	$^{206}Pb/^{238}U$	±	$^{207}Pb/^{206}Pb$	±	$^{206}Pb/^{238}U$	±	$^{207}Pb/^{206}Pb$
1	300	0.3053	0.0071	0.03315	0.00047	0.58385	0.0657	0.0011	270.5	5.6	210.2	2.9	791	34	206.2	2.9	0.84941
2	210	0.3549	0.0081	0.03398	0.00045	0.47009	0.0743	0.0014	308.4	6.0	215.4	2.8	1040	38	209.0	2.8	0.84976
3	191	0.3375	0.0069	0.04679	0.00120	0.70849	0.05214	0.00067	295.3	5.2	294.8	7.2	288	30	294.8	7.5	0.85518
4	213	0.3041	0.0070	0.03230	0.00043	0.2096	0.0676	0.0015	269.6	5.6	204.9	2.7	857	45	200.5	2.7	0.84906
5	128	0.2301	0.0047	0.03302	0.00070	0.44182	0.0499	0.00097	210.3	3.9	209.4	4.4	181	43	209.5	4.4	0.84936
6	102	0.2613	0.0083	0.03437	0.00073	0.41152	0.0549	0.0016	235.7	6.6	217.9	4.5	397	61	216.7	4.6	0.84993
7	164	0.3180	0.0083	0.03509	0.00081	0.56781	0.0664	0.0013	280.4	6.4	222.3	5.0	826	42	218.0	5.0	0.85023
9	190	0.2682	0.0093	0.03620	0.00095	0.762	0.0537	0.0014	241.3	7.3	229.3	5.9	346	57	228.4	5.9	0.85070
10	338	0.2286	0.0053	0.03311	0.00084	0.78905	0.05064	0.00061	209.1	4.3	210.0	5.2	224	28	209.9	5.3	0.84940
11	128	0.2382	0.0061	0.03406	0.00086	0.68568	0.0514	0.001	216.9	4.9	215.9	5.3	250	45	215.7	5.4	0.84980
12	74	0.2299	0.0064	0.03280	0.00070	0.516	0.0502	0.0011	210.1	5.2	208.0	4.3	203	49	208.1	4.4	0.84927
13	303	0.3412	0.0100	0.03433	0.00076	0.44353	0.0701	0.0018	298.1	7.6	217.6	4.7	941	53	212.3	4.7	0.84991
14	232	0.2399	0.0053	0.03365	0.00086	0.67652	0.05127	0.00081	218.3	4.3	213.3	5.4	251	36	213.1	5.4	0.84962
15	135	0.2704	0.0083	0.03458	0.00079	0.50964	0.0554	0.0012	243.0	6.6	219.2	4.9	416	45	217.8	4.9	0.85002
16	146	0.2414	0.0047	0.03393	0.00073	0.61406	0.05045	0.00082	219.6	3.8	215.1	4.5	210	36	215.1	4.6	0.84974
17	170	0.3351	0.0088	0.03286	0.00089	0.6721	0.072	0.0014	293.5	6.6	208.4	5.5	993	40	202.8	5.4	0.84929
18	80	0.3517	0.0097	0.03663	0.00083	0.712	0.0683	0.0012	306.0	7.2	231.9	5.1	878	39	226.9	5.1	0.85088
19	90	0.3373	0.0083	0.04698	0.00100	0.77526	0.0527	0.00086	295.1	6.3	295.9	6.3	310	37	295.8	6.2	0.85526
23	198	0.2298	0.0048	0.03341	0.00070	0.70905	0.05042	0.00081	210.1	3.9	211.9	4.3	209	37	211.9	4.4	0.84952
24	251	0.2311	0.0045	0.03337	0.00071	0.7168	0.0507	0.0008	211.1	3.6	211.6	4.4	220	35	211.5	4.5	0.84951
26	232	0.3455	0.0086	0.04698	0.00120	0.62917	0.05209	0.00094	301.3	6.5	295.9	7.4	283	42	296.0	7.5	0.85526
27	362	0.2408	0.0043	0.03382	0.00067	0.78016	0.05074	0.00054	219.1	3.6	214.4	4.2	228	25	214.3	4.2	0.84970
28	135	0.4872	0.0170	0.04811	0.00100	0.47072	0.0717	0.0023	403.0	11.0	302.9	6.4	989	66	295.7	6.1	0.85575
29	324	0.2427	0.0063	0.03358	0.00100	0.73534	0.05133	0.0009	220.7	5.0	212.9	6.2	254	41	212.7	6.3	0.84960
30	293	0.2437	0.0045	0.03306	0.00068	0.56062	0.05284	0.00081	221.4	3.7	209.7	4.2	314	35	209.0	4.3	0.84938
31	61	0.3309	0.0081	0.04584	0.00100	0.50409	0.0519	0.0011	290.2	6.1	289.0	6.2	273	47	289.0	6.2	0.85478
32	431	0.3407	0.0054	0.04664	0.00083	0.67283	0.05325	0.00058	297.7	4.0	293.8	5.0	338	25	293.5	5.2	0.85512
33	422	0.2322	0.0053	0.03302	0.00067	0.74822	0.05128	0.00072	212.0	4.3	209.4	4.2	251	33	209.1	4.2	0.84936
34	151	0.2464	0.0140	0.03471	0.00150	0.52482	0.0517	0.0021	223.7	11.0	220.0	9.5	257	88	219.7	9.4	0.85007
36	173	0.2422	0.0053	0.03474	0.00063	0.66374	0.05061	0.00081	220.2	4.4	220.2	3.9	216	36	220.1	4.0	0.85009
37	175	0.2518	0.0080	0.03268	0.00051	0.4735	0.0559	0.0014	228.1	6.4	207.3	3.2	438	52	205.8	3.2	0.84922
38	137	0.2394	0.0061	0.03303	0.00071	0.62493	0.05207	0.00098	217.9	4.9	209.5	4.4	279	43	209.1	4.5	0.84937

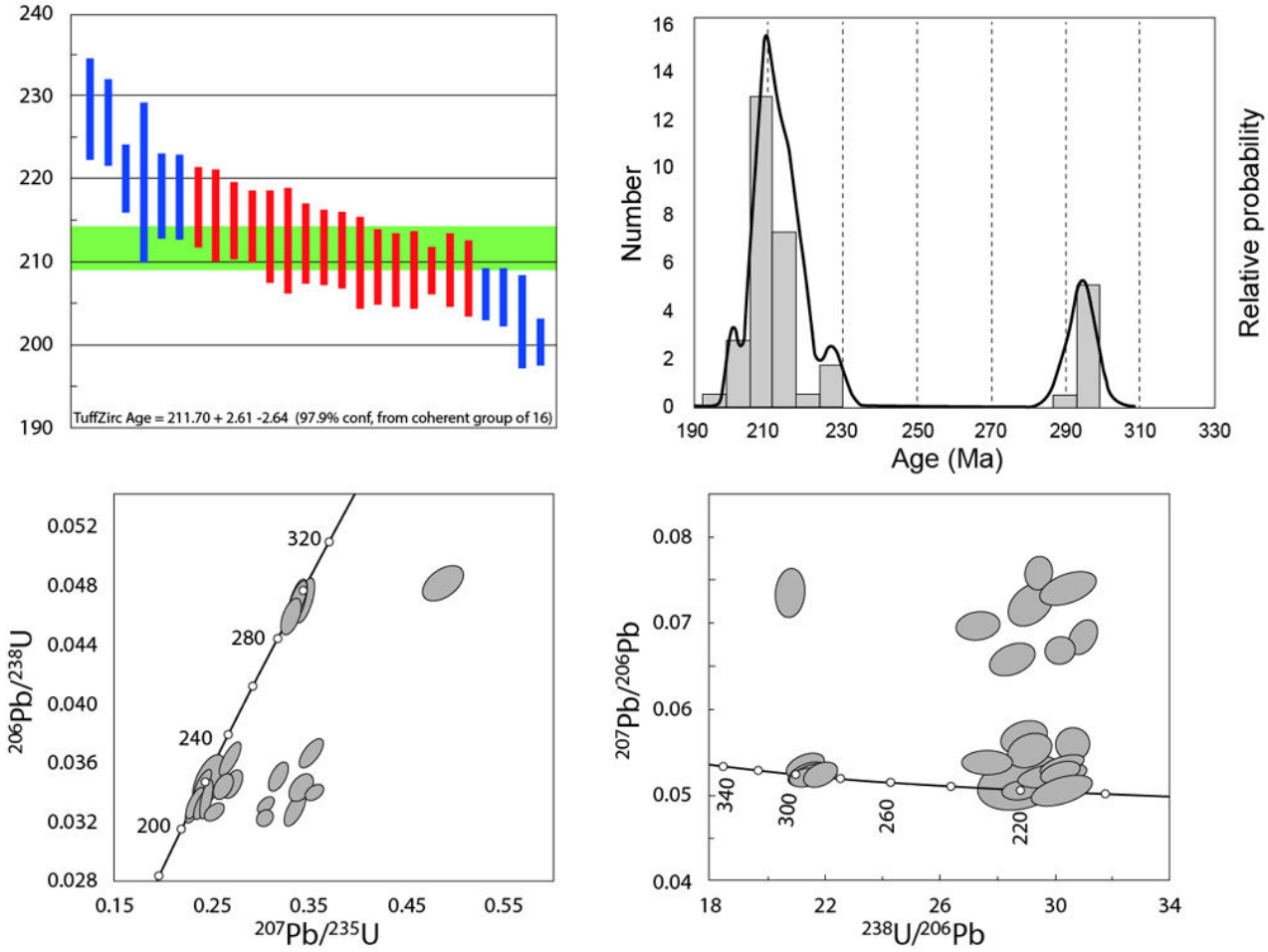

Figure 10: Radiogenics ages of sample LMM-6.

- Late Triassic subaqueous volcanism-near-arc basin. Hydrovolcanic deposits as well as breccias with subaerial volcanic ejecta are identified in the upper levels of the Pichidangui Formation and in facies association E of the El Puquén Formation. These beds are interpreted as products of basaltic-andesitic-dacitic lava domes emplaced in a subaqueous environment with a carapace of hyaloclastites and peperites. Therefore, the identification of subaqueous hydrovolcanic facies and bombs in these units, indicative of both subaquatic and subaerial volcanism, suggests surtseyan volcanism, supporting the hypothesis presented by Ibáñez (2021). A near-arc setting, likely within an intra-arc basin, is inferred for the El Puquén Formation. Conversely, the general absence of pyroclastic detritus in the Los Molles Formation may be explained by considering a prevailing wind direction from the ocean to the continent, with the volcanoes to the east, suggesting a fore-arc setting for this formation. This is supported by the north-south belt of Late Triassic to Early Jurassic plutonic rocks (Mincha Superunit; Brook *et al.*, 1986; Rivano & Sepúlveda, 1993) exposed to the east and north of the El Puquén and Los Molles formations, which are considered to be the roots of coeval volcanos.

- Continuous intermittent volcanism. Volcanism persisted during the deposition of almost all facies associations (fa) of the El Puquén Formation: air-fall deposits are intercalated throughout the formation, indicating that volcanic activity continued intermittently, either in a diminished capacity or at a greater distance from the volcanic centres. The following are the main volcanic intercalations in this formation: in faA, turbidites with pyroclasts; in faB, ash layer intercalations; in faD, pyroclastic flow mixing with lake-bottom shales and sandstones; in faE, peperites suggesting a nearby volcano; in faF, hyaloclastites and bombs; in faG, lapilli-fall deposits intercalated within the sandstones and shales. This volcanism is a continuation, although less intense, of that observed in the Pichidangui Formation. However, volcanic intercalations were absent during the Late Triassic to earliest Jurassic deposition of the Los Molles Formation.

- Synsedimentary extensional tectonism: Scissor-type graben and small faults. A WNW synsedimentary graben and small healed post-graben normal faults identified in facies associations A and B suggest that, for at least part of the Rhaetian, extensional faults controlled the development of the El Puquén sedimentary basin. Although this graben implies limited tectonic extension, it may be interpreted as a fractal representation and the first field evidence supporting the hypothesis of Late Triassic extensional tectonism in the studied region (see Charrier, 1979; Suárez & Bell, 1992; Suarez *et al.*, 2010).

- Seismic activity during accumulation of the El Puquén Formation. In addition to the syntectonic extensional faults, numerous other soft-sediment structures formed during and/or after sedimentation and before complete lithification are common features, particularly in facies association C of the El Puquén Formation. These soft-sediment features include slumps, clastic dikes (probably formed due to overpressure from slumped vertically stacked sediments and seismic activity), synsedimentary breccias, convolute bedding, and load casts. The triggering process may have involved seismic activity related to both deep-seated seismicity associated with subduction processes and shallow-level seismicity related to active volcanism. In some cases, seismicity may have generated mass flows that introduced additional weight onto the existing basin floor sediments.

- The tectonic setting during the Triassic to Jurassic. One of the prevailing hypotheses on the Permian to Mesozoic tectonic evolution of the Southern Andes is that there was a major breakup at the end of the Triassic, with the recognition of a pre-Andean (early Permian to late Triassic) and an Andean cycle (that began in the late Triassic; *e.g.*, Charrier *et al.*, 2007). The main argument was that these cycles differ mostly in their magmatic history and tectonic regime: the pre-Andean cycle was interpreted as a period of arrested subduction and the development of a continental rift along the southwestern margin of Gondwana, but, new geochemical studies indicate that during the time span of the pre-Andean cycle, subduction was an active process and that the bimodal volcanism of the Triassic Pichidangui Formation in the area of this study also indicates that subduction processes were active in the Triassic, during pre-Andean times (Coloma *et al.*, 2017; Oliveros *et al.*, 2020; Ibáñez, 2021). Furthermore, as indicated herein, there is no major tectonic change during the accumulation of the Late Triassic to Early Jurassic Los Molles Formation (except for a change from fan-delta deposition, probably during a highstand systems tracts and/or tectonism, to slope apron deposits and finally to submarine fan sediments during a lowstand sea-level period (in prep.).

Acknowledgements

This work was supported by the Universidad Andrés Bello, the Servicio Nacional de Geología y Minería and Fondecyt 511-90. We thank Bastián Oyanedel for the drawings.

Bibliographic references

Azcárate V. & Fasola A. (1970).- Sobre formas nuevas para la flora triásica de Los Molles.- *Boletín del Museo Nacional de Historia Natural*, Santiago de Chile, vol. 29, p. 249-269.

Bell C.M. & Suárez M. (1995).- Slope apron deposits of the Lower Jurassic Los Molles Formation, Central Chile.- *Revista Geológica de Chile*, Santiago de Chile, vol. 22, no. 1, p. 103-114. URL: https://dialnet.unirioja.es/servlet/articulo?codigo=6680830

Brook M., Pankhurst R., Shepard T. & Spiro B. (1986, unpublished).- ANDCHRON : Andean geochronology and metallogenesis. Final report for the Overseas Development Administration Research and Development Project on the application of geochronology, isotope geology and fluid inclusion studies to understanding the geological evolution of the Southern Andes and the setting and formation of metallic ore deposits therein.- British Geological Survey, London, 137 p. URI: https://nora.nerc.ac.uk/id/eprint/523045

Cancino A. (1992, unpublished).- Contribución a la petrología e interpretación tectónica de las rocas volcánicas triásicas y jurásicas de la región central de Chile (33°-34° Lat. S).- Memoria de Título, Universidad de Chile, Santiago de Chile, 259 p.

Cecioni G. & Westermann G.E.G. (1968).- The Triassic Jurassic marine transition of Coastal Central Chile.- *Pacific Geology*, Tokyo, vol. 1, p. 41-75. URL: https://bibliotecadigital.ciren.cl/handle/20.500.13082/12958

Charrier R. (1979).- El Triásico en Chile y regiones adyacentes de Argentina - Una reconstrucción paleogeográfica y paleoclimática.- *Comunicaciones*, *Universidad de Chile*, Santiago de Chile, vol. 26, p. 1-47.

Charrier R., Contreras J.P., Díaz-Bórquez D., Farías M., Jara P., Muñoz-Gómez M., Quiñones S., Rodríguez M.P., Tapia F. & Villaseñor T. (2024).- The Cenozoic Abanico rift system: Implications of increased southward extension in the southern central Andes, in Chile.- *Journal of South American Earth Sciences*, vol. 148, article 105149, 17 p.

Charrier R., Pinto L. & Rodriguez M.P. (2007).- Tectonostratigraphic evolution of the Andean Orogen in Chile. *In*: Moreno T. & Gibbons W. (eds.), The geology of Chile.- *Geology of series*, *Geological Society*, London, p. 21-114.

Charrier R., Ramos V., Tapia F. & Sagripanti L. (2014).- Tectono-stratigraphic evolution of the Andean Orogen between 31 and 37°S (Chile and Western Argentina).- *Special Publications*, *Geological Society*, London, vol. 399, p. 13-61.

Coloma F., Valin X., Oliveros V., Vásquez P., Creixell C., Salazar E. & Ducea M.N. (2017).- Geochemistry of Permian to Triassic igneous rocks from northern Chile (28°-30°15'S): Implications on the dynamics of the proto-Andean margin.- *Andean Geology*, Santiago de Chile, vol. 44, no. 2, p. 147-178. URL: https://dialnet.unirioja.es/servlet/articulo?codigo=6163425

Covacevich V., Suárez M. & Sepúlveda P. (1987).- Trazas fósiles de crustáceos decápodos en el Triasico Superior de la Formacion Los Molles (Chile Central): Nueva evidencia indicativa de facies de mar somero.- *Revista Geológica de Chile*, Santiago de Chile, vol. 30, p. 19-25. URL: https://dialnet.unirioja.es/servlet/articulo?codigo=6158151

ESPIÑEIRA D. (1989, unpublished).- Geología del Complejo Plutónico Papudo-Quintero: Aspectos cronológicos y geoquímicos.- Memoria de Título, Universidad de Chile, Santiago de Chile, 146 p.

FUENZALIDA V.H. (1938).- Las capas de Los Molles.- *Boletín del Museo nacional de Historia natural*, Santiago de Chile, vol. 16, p. 66-92. DOI: https://doi.org/10.54830/bmnhn.v16.1937.714

GONZÁLEZ J., OLIVEROS V., CREIXELL C., VELÁSQUEZ R., VÁSQUEZ P. & LUCASSEN F. (2018).- The Triassic magmatism and its relation with the Pre-Andean tectonic evolution: Geochemical and petrographic constrains from the High Andes of north central Chile (29°30' - 30°S).- *Journal of South American Earth Sciences*, vol. 87, p. 95-112.

HERBST R. & TRONCOSO A. (2014).- Las Cycadophyta del Triásico de las Formaciones La Ternera y El Puquén (Chile).- *Ameghiniana*, Buenos Aires, vol. 37, no. 3, p. 283-292.

IBÁÑEZ V. (2021, unpublished).- Caracterización de las paleofacies volcánicas de la Formación Pichidangui, sector El Puquén, Los Molles, Chile.- Memoria de título, Universidad Andrés Bello, 98 p.

MELCHOR R.N. & HERBST R. (2000).- Sedimentology of the El Puquén Formation (Upper Triassic, central Chile) and the new plant *Mollesia melendeziae* gen. et sp. nov. (Pteridophylla, *incertae sedis*).- *Ameghiniana*, Buenos Aires, vol. 37, no. 4, p. 477-485.

MELCHOR R.N. & HERBST R. (2003).- Sedimentology and paleobotany of the El Puquén Formation (Upper Triassic), central Chile.- *Ameghiniana*, Buenos Aires, vol. 40, no. 4, p. 487-505.

MELO C. (2020, unpublished).- Estratigrafia y sedimentologia de los niveles basales de la Formacion los Molles, Los Molles, Region de Valparaiso, Chile.- Memoria de título, Universidad Andrés Bello, 93 p.

MORATA D., AGUIRRE L., OYARZUN M. & VERGARA M. (2000).- Crustal contribution in the genesis of the bimodal Triassic volcanism from the Coastal Range, central Chile.- *Revista Geológica de Chile*, Santiago de Chile, vol. 27, no. 1, p. 83-98. URL: https://dialnet.unirioja.es/servlet/articulo?codigo=6158364

MUNIZAGA F. (1972).- Edades radiométricas de rocas Chilenas. *In*: Jornadas de Trabajo.- Instituto de Investigaciones Geológicas, Antofagasta, vol. 2, sec. 1, p. 132-145.

NASI PRADO C., MPODOZIS C., CORNEJO PELÁEZ P., MOSCOSO DÍAZ R. & MAKSAEV V. (1985).- El Batolito Elqui-Limari (Paleozoico superior-Triásico): Características petrográficas, geoquímicas y significado tectónico.- *Revista Geológica de Chile*, Santiago de Chile, vol. 25-26, p. 77-111. URL: https://dialnet.unirioja.es/servlet/articulo?codigo=6158208

OLIVEROS O., VÁSQUEZ P., CREIXELL C., LUCASSEN F., DUCEA M.N., CIOCCA I., GONZÁLEZ J., ESPINOZA M., SALAZAR E., COLOMA F. & KASEMANN S.A. (2020).- Lithospheric evolution of the Pre- and Early Andean convergent margin, Chile.- *Gondwana Research*, vol. 80, p. 202-227.

PARADA M., RIVANO S., SEPÚLVEDA P., HERVÉ M., HERVÉ F., PUIG A., MUNIZAGA F., BROOK M., PANKHURST R. & SNELLING N. (1988).- Mesozoic and Cenozoic plutonic development in the Andes Central Chile (30°30'-31°30').- *Journal of South American Earth Sciences*, vol. 1, no. 3, p. 249-260.

RIVANO S. & SEPÚLVEDA P. (1991).- Hoja Illapel. Región de Coquimbo.- *Carta Geológica de Chile*, Servicio Nacional de Geología y Minería, Santiago de Chile, no. 69, 1 mapa 1:250.000.

RIVANO S., SEPÚLVEDA P., BORIC R. & ESPIÑEIRA D. (1993).- Hojas Quillota y Portillo.- *Carta Geológica de Chile*, Servicio Nacional de Geología y Minería, Santiago de Chile, no. 73, 1 mapa 1:250.000.

STEIGER R.H. & JÄGER E. (1977).- Subcommission on geochronology: Convention on the use of decay constants in geo- and cosmochronology.- *Earth and Planetary Science Letters*, vol. 36, no. 3, p. 359-362.

STIPANICIC P.N. (1983).- The Triassic of Argentina and Chile*. In*: MOULLADE M. & NAIRN A.E.M. (eds.), The Phanerozoic geology of the world. The Mesozoic, B.- Elsevier, Amsterdam, p. 181-199.

STIPANICIC P.N. (2001).- Antecedentes geológicos y paleontológicos. *In*: ARTABE A.E., MOREL E.M. & ZAMUNER A.B. (eds.), El sistema Triásico de Argentina.- Fundación Museo de La Plata "Francisco Pascasio Moreno", La Plata, p. 1-21.

SUÁREZ M. & BELL C.M. (1992).- Triassic rift-related sedimentary basins in northern Chile (24°-29°S).- *Journal of South American Earth Sciences*, vol. 6, no. 3, p. 109-121.

SUÁREZ M., DE LA CRUZ R., BELL C.M. & DEMANT A. (2010).- Cretaceous slab segmentation in southwestern Gondwana.- *Geological Magazine*, Cambridge (UK), vol. 147, no. 2, p. 193-205.

SUÁREZ M., GRESSIER J.B., DESCOTE P-Y. & DE LA CRUZ R. (2018).- Tectonismo extensional y volcanismo Nórico (Triásico tardío) en Chile Central: Edades U-Pb.- ESEG-2, Actas XV Congreso Geológico Chileno, Concepción, 1 p. (abstract).

TRONCOSO A. & HERBST R. (1999).- Las Ginkgoales del Triásico del Norte Chico de Chile.- *Revista Geológica de Chile*, Santiago de Chile, vol. 26, no. 2, p. 255-273. URL: https://dialnet.unirioja.es/servlet/articulo?codigo=6158259

VERGARA M., LEVI B., NYSTRÖM J.O. & CANCINO A. (1995).- Jurassic and Early Cretaceous island arc volcanism, extension and subsidence in the Coast Range of central Chile.- Geological Society of America, *Bulletin*, Boulder - CO, vol. 107, no. 12, p. 1427-1440.

VERGARA M., LÓPEZ-ESCOBAR L. & CANCINO A. (1991).- The Pichidangui Formation: Some geochemical characteristics and tectonic implications of the Triassic marine volcanism in central Chile (31°55' to 32°20'S).- *Geological Society of America*, *Special Paper*, Boulder - CO, vol. 265, p. 93-98.

VICENTE J.C. (1976).- Exemple de "volcanisme initial euliminaire" : Les complexes albitophyriques néo-triasiques et mésojurassiques du secteur côtier des Andes Méridionales centrales (32° à 33° L. Sud). *In*: GONZÁLEZ-FERRÁN O. (ed.), Proceedings of the Symposium on Andean and Antarctic Volcanolgy Problems.- International Association of Volcanology and Chemistry of the Earth's Interior, Special Series, Napoli, p. 267-329.